

Macromolecular Materials and Engineering

A Comparison of Electric-Field-driven and Pressure-driven Fiber Generation Methods for Drug Delivery --Manuscript Draft--

Manuscript Number:	name.201700577R1
Full Title:	A Comparison of Electric-Field-driven and Pressure-driven Fiber Generation Methods for Drug Delivery
Article Type:	Full Paper
Section/Category:	
Keywords:	pressure; gyration; electrospinning; fibers; drug delivery
Corresponding Author:	Mohan Edirisinghe, Prof. University College London London, London UNITED KINGDOM
Corresponding Author Secondary Information:	
Corresponding Author's Institution:	University College London
Corresponding Author's Secondary Institution:	
First Author:	Mohan Edirisinghe, Prof.
First Author Secondary Information:	
Order of Authors:	Mohan Edirisinghe, Prof. Jubair Ahmed, MSc, BSc Rupy Kaur Matharu, MSc, BSc Talayah Shams, MSc, BSc Upulitha Eranka Illangakoon, Phd,MSc,BSc
Order of Authors Secondary Information:	
Abstract:	<p>Polymeric fibers were prepared by using electric field driven fiber production technology - electrospinning and pressure driven fiber production technology - pressurised gyration. Fibers of four different polymers: polyvinylidene fluoride (PVDF), poly(methyl methacrylate (PMMA), poly(N-isopropylacrylamide) (PINIPAAM) and polyvinylpyridine (PVP), were spun by both techniques and differences were analysed for their suitability as drug carriers. The diameters of electrospun fibers were larger in some cases (PVDF and PMMA), producing fibers with lower surface area. Pressurised gyration allowed for a higher rate of fiber production. Additionally, drug-loaded PVP fibers were prepared by using two poorly water-soluble drugs (Amphotericin B and Itraconazole). In-vitro dissolution studies show differences in release rate between the two types of fibers. Drug- loaded gyrospun fibers release the drugs faster within 15 minutes compared to the drug-loaded electrospun fibers. The findings suggest pressurised gyration is a promising and scalable approach to rapid fiber production for drug delivery when compared to electrospinning.</p>
Additional Information:	
Question	Response
Please submit a plain text version of your cover letter here. Please note, if you are submitting a revision of your manuscript, there is an opportunity for you to provide your responses to the reviewers later; please	See Response document

do not add them to the cover letter.	
Do you or any of your co-authors have a conflict of interest to declare?	No. The authors declare no conflict of interest.

A Comparison of Electric-Field-driven and Pressure-driven Fiber Generation Methods for Drug Delivery.

Jubair Ahmed, Rupy Kaur Matharu, Talayeh Shams, Upulitha Eranka Illangakoon, Mohan Edirisinghe*

J. Ahmed. MSc., R.K. Matharu. MSc., T. Shams. MSc., Dr. U.E. Illangakoon PhD., Prof. M. Edirisinghe DSc.

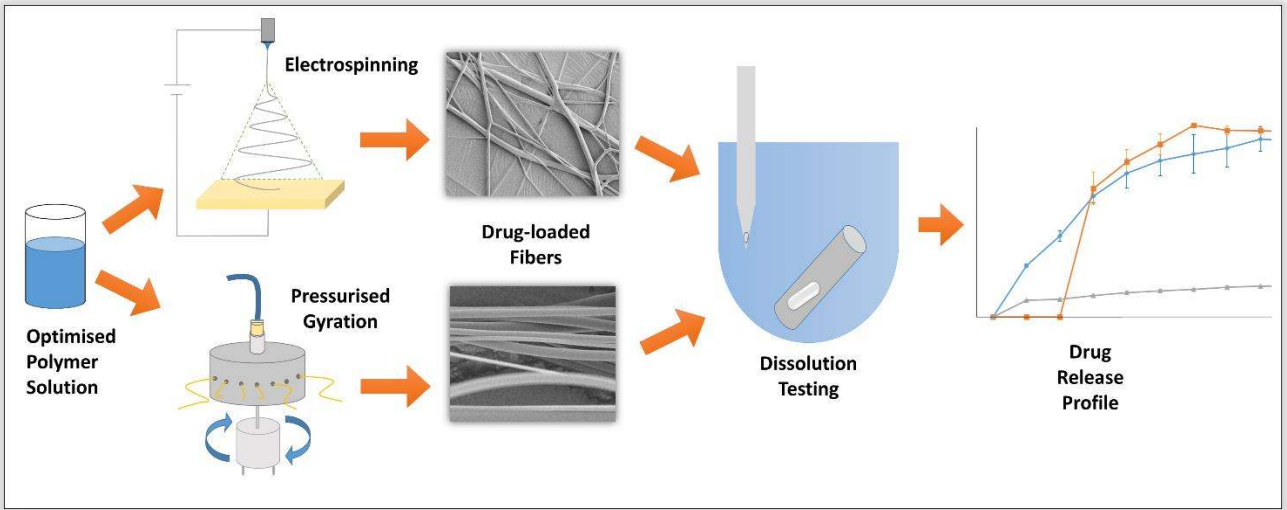
Department of Mechanical Engineering, University College London, Torrington Place, London WC1E 7JE, United Kingdom

* Corresponding author: m.edirisinghe@ucl.ac.uk

Polymeric fibers were prepared by using electric field driven fiber production technology – electrospinning and pressure driven fiber production technology – pressurised gyration. Fibers of four different polymers: polyvinylidene fluoride (PVDF), poly(methyl methacrylate (PMMA), poly(N-isopropylacrylamide) (PINIPAAM) and polyvinylpyridine (PVP), were spun by both techniques and differences were analysed for their suitability as drug carriers. The diameters of electrospun fibers were larger in some cases (PVDF and PMMA), producing fibers with lower surface area. Pressurised gyration allowed for a higher rate of fiber production. Additionally, drug-loaded PVP fibers were prepared by using two poorly water-soluble drugs (Amphotericin B and Itraconazole). In-vitro dissolution studies show differences in release rate between the two types of fibers. Drug- loaded gyrosun fibers release the drugs faster within 15 minutes compared to the drug-loaded electrospun fibers. The findings suggest pressurised gyration is a promising and scalable approach to rapid fiber production for drug delivery when compared to electrospinning.

Keywords: (pressure; gyration; electrospinning; fibers; drug delivery)

1
2
3
4
5
6
7
8
9
10
11
12
13
14
15
16
17
18
19
20
21
22
23
24
25
26
27
28
29
30
31
32
33
34
35
36
37
38
39
40
41
42
43
44
45
46
47
48
49
50
51
52
53
54
55
56
57
58
59
60
61
62
63
64
65



1. Introduction

1
2
3 Interest in fibers, at both the micro and nano-scale has not conveyed any slowdown in recent
4
5 years. Fiber production continues to be an area of soaring interest in both the academic and
6
7 industrial fields. The global market for nanofibers reached a staggering \$383.7 million in 2015
8
9 and is projected to approach \$2 billion by 2020 ^[1].

10
11
12 The sheer versatility of such fibers, allows them to be exploited in a multitude of applications
13
14 including: biomaterials, tissue engineering, textiles, sensors, wound healing and moreover drug
15
16 delivery ^[2-4]. It is the inherent compact nature of these small diameter fibers that unravels many
17
18 astonishing and undeniably beneficial characteristics. As the diameters of these fibers are
19
20 reduced below the micrometre scale (1-100 μm): features corresponding to enormously high
21
22 surface area to volume ratio, superior mechanical properties and tailorable surface
23
24 functionalization become increasingly apparent ^[5]. For these reasons and many others to be
25
26 explored, small diameter fibers are remarkably suited for the range of functional applications
27
28 that they are exploited in.
29
30
31
32
33

34
35 The production of small-diameter fibers is thus a key area for research and development.
36
37 Improving upon the yield, efficiency, and control in manufacturing will inevitably speed the
38
39 advancement of these valuable materials. Until only recently, there has been a single tried and
40
41 tested method for laboratory fiber production. The exploration and comparison with novel
42
43 methods of fiber production serves to evolve the field of fiber production as there are several
44
45 shortcomings and downfalls that exist for the current “gold standard”, electrospinning (ES),
46
47 which has been widely recognised as a simple, versatile and facile method for the fabrication
48
49 of polymeric fibers with a wide range of uses including drug delivery ^[5, 6]. However, there are
50
51 inherent limitations to this technology that impede its ability to upscale production to meet the
52
53 ever-increasing demand on micro- and nano-scaled materials. Furthermore, the use of fine
54
55 tubing produces problems of solution and needle clogging, which reduces production yield and
56
57 increases maintenance costs ^[7].
58
59
60
61
62

1 A novel pressure driven route for the production of fibers was reported in 2013 and has been
2 improved further incorporate simultaneous use of pressure, flow and rotation ^[8,9]. The process
3 known as pressurised gyration (PG), marries centrifugal spinning with solution blow spinning.
4 Pressure-driven nanofiber production methods such as pressurised gyration, offer a compelling
5 alternative to electric-field driven technologies such as electrospinning. This comes with the
6 ability to spin charge-absent polymers and potentially improve production yield. In essence,
7 centrifugal spinning involves a perforated spinneret to which a polymer solution is fed into and
8 then rotated at high speeds. Upon reaching a critical rotational speed, the solution is forced out
9 of the perforations and deposited as dry nanofibers following solvent evaporation ^[9, 10].
10 Conversely, solution blow spinning is an alternative nanofiber production route which
11 implicates a high velocity gas flow to a polymer solution. The pressurised gas extrudes and
12 drives the polymer solution to cause rapid solvent evaporation, generating dried fibers in a
13 simple one-step process ^[11].

14 Polyvinylpyrrolidone (PVP), is a hydrophilic polymer of N-vinylpyrrolidone^[12]. In their history
15 spanning over 70 years, vinylpyrrolidone polymers have seen extensive use in technical
16 applications, food packaging, cosmetics and especially in pharmaceuticals where it is used as a
17 disintegrant or tablet binder ^[13]. Furthermore, due to its profound ability to readily dissolve in
18 water and oil; PVP has been used as a vehicle for suspending and dispersing drugs ^[14].

19 Polyvinylidene fluoride (PVDF), is a non-reactive thermoplastic commonly used as insulation
20 material for electrical wires but has promising use in biomedical applications such as
21 hemodialysis filtration ^[15]. Poly (methyl methacrylate) (PMMA), is a biodegradable transparent
22 thermoplastic which sees frequent use as bone cement in joint replacement surgeries ^[16].

23 Poly(N-isopropylacrylamide) (PNIPAm), is a temperature-responsive polymer with a wide
24 range of applications ranging from biosensors, tissue engineering and drug delivery ^[17].

25 Thermo-responsive core-sheath nanofibres have been prepared by electrospinning but literature
26 with other fibre-production methods is scarce ^[18].

1
2
3
4 A comparison in the fiber morphology, accessibility and final product performance (drug
5 delivery) has yet to be completed. The importance of this study is to assess the formation of
6 fibres from two fundamentally different techniques to determine any differences in product
7 performance in terms of drug delivery. As pressurised gyration offers the advantage of
8 potential scale up: the proposition of this study was to compare the fiber production of
9 electrospinning and pressurised gyration on the product morphology, production efficiency and
10 drug release capability. For this purpose, four different polymers were selected: namely
11 Polyvinylpyrrolidone (PVP), Polyvinylidene fluoride (PVDF), Poly(methyl methacrylate)
12 (PMMA) and Poly(*N*-isopropylacrylamide) (PINIPAAM). Production of fine diameter fibers
13 are beneficial towards drug release as finer fibers afford a higher surface area to volume ratio,
14 which can improve drug dissolution [19]. Therefore, PVP Fibers are compared in their ability to
15 improve the oral dissolution of a poorly soluble drug, amphotericin B (AMB) and itraconazole
16 (ITZ).
17
18
19
20
21
22
23
24
25
26
27
28
29
30
31
32
33
34
35

36 2. Materials and Methods

37
38
39 PVP (Mw 1,300,000 g mol⁻¹), PVDF (Mw 275,000 g mol⁻¹), PMMA solution (Mw 120,000 g
40 mol⁻¹), PNIPAm (Mw 300,000 g mol⁻¹), itraconazole (CAS: 84625-61-6; ITZ) and
41 amphotericin B (CAS: 1397.89.3; AMB) were obtained from Sigma-Aldrich (Gillingham, UK).
42 Solvents used are summarised in **Table 1**: Ethanol (CAS: 64-17-5), Dimethylformamide (CAS:
43 68-12-2), Acetone (CAS: 67-64-1) and Chloroform (CAS: 67-66-3), all of which were acquired
44 from Sigma-Aldrich (Gillingham, UK).
45
46
47
48
49
50
51
52
53
54

55 2.1. Preparation of spinning solutions and spinning conditions

1 The polymer solutions used in this study are listed in **Table 1**. Each polymer solution was
2 prepared by adding the specific amount of polymer to the solvent and mechanically stirred for
3
4 24 hours at $24^{\circ}\text{C} \pm 3^{\circ}\text{C}$ to obtain a homogeneous polymer solution.
5
6

7 8 2.1.1. Solution Characterisation 9

10
11 Surface tension of the prepared solutions were characterised via a tensiometer (Tensiometer
12 K9, Kruss GmbH, Germany) and were repeated 5 times to find the average surface tension.
13

14
15 Viscosity was characterised using a programmable rheometer (DV-III Ultra, Brookfield
16 Engineering Laboratories INC, Massachusetts, USA), readings were taken at a shear stress of
17
18
19 ~ 5 Pa, **measurements were repeated 3 times to find the average value.**
20
21
22
23

24 25 2.1.2. Electrospinning 26

27
28 A schematic diagram of the electrospinning setup is shown in **Figure 1 (a)** and the spinning
29 solutions were carefully placed into a plastic syringe (10 mL, (BD Plastic™, VWR,
30 Lutterworth, UK), great care taken to avoid any air bubbles. A metal dispensing tip (spinneret;
31 inner diameter: 2.03 mm, outer diameter: 1.52mm Stainless Tube & Needle Co Ltd., Tamworth,
32 UK) was attached to the syringe. The polymer solution was dispensed from the syringe at a feed
33 rate of 1.2 mL/h using a syringe pump (PHD 4400, Harvard Apparatus, Edenbridge, UK). The
34 positive electrode of a high voltage power DC supply (Glassman Europe Ltd., Tadley, UK) was
35 then connected to the spinneret. The grounded electrode was connected to a metal collector
36 wrapped with aluminium foil. Electrospinning was carried out under ambient conditions ($23 \pm$
37
38
39
40
41
42
43
44
45
46
47
48
49
50
51
52
53
54
55
56
57
58
59
60
61
62
63
64
65
66
67
68
69
70
71
72
73
74
75
76
77
78
79
80
81
82
83
84
85
86
87
88
89
90
91
92
93
94
95
96
97
98
99
100
101
102
103
104
105
106
107
108
109
110
111
112
113
114
115
116
117
118
119
120
121
122
123
124
125
126
127
128
129
130
131
132
133
134
135
136
137
138
139
140
141
142
143
144
145
146
147
148
149
150
151
152
153
154
155
156
157
158
159
160
161
162
163
164
165
166
167
168
169
170
171
172
173
174
175
176
177
178
179
180
181
182
183
184
185
186
187
188
189
190
191
192
193
194
195
196
197
198
199
200
201
202
203
204
205
206
207
208
209
210
211
212
213
214
215
216
217
218
219
220
221
222
223
224
225
226
227
228
229
230
231
232
233
234
235
236
237
238
239
240
241
242
243
244
245
246
247
248
249
250
251
252
253
254
255
256
257
258
259
260
261
262
263
264
265
266
267
268
269
270
271
272
273
274
275
276
277
278
279
280
281
282
283
284
285
286
287
288
289
290
291
292
293
294
295
296
297
298
299
300
301
302
303
304
305
306
307
308
309
310
311
312
313
314
315
316
317
318
319
320
321
322
323
324
325
326
327
328
329
330
331
332
333
334
335
336
337
338
339
340
341
342
343
344
345
346
347
348
349
350
351
352
353
354
355
356
357
358
359
360
361
362
363
364
365
366
367
368
369
370
371
372
373
374
375
376
377
378
379
380
381
382
383
384
385
386
387
388
389
390
391
392
393
394
395
396
397
398
399
400
401
402
403
404
405
406
407
408
409
410
411
412
413
414
415
416
417
418
419
420
421
422
423
424
425
426
427
428
429
430
431
432
433
434
435
436
437
438
439
440
441
442
443
444
445
446
447
448
449
450
451
452
453
454
455
456
457
458
459
460
461
462
463
464
465
466
467
468
469
470
471
472
473
474
475
476
477
478
479
480
481
482
483
484
485
486
487
488
489
490
491
492
493
494
495
496
497
498
499
500
501
502
503
504
505
506
507
508
509
510
511
512
513
514
515
516
517
518
519
520
521
522
523
524
525
526
527
528
529
530
531
532
533
534
535
536
537
538
539
540
541
542
543
544
545
546
547
548
549
550
551
552
553
554
555
556
557
558
559
560
561
562
563
564
565
566
567
568
569
570
571
572
573
574
575
576
577
578
579
580
581
582
583
584
585
586
587
588
589
590
591
592
593
594
595
596
597
598
599
600
601
602
603
604
605
606
607
608
609
610
611
612
613
614
615
616
617
618
619
620
621
622
623
624
625
626
627
628
629
630
631
632
633
634
635
636
637
638
639
640
641
642
643
644
645
646
647
648
649
650
651
652
653
654
655
656
657
658
659
660
661
662
663
664
665
666
667
668
669
670
671
672
673
674
675
676
677
678
679
680
681
682
683
684
685
686
687
688
689
690
691
692
693
694
695
696
697
698
699
700
701
702
703
704
705
706
707
708
709
710
711
712
713
714
715
716
717
718
719
720
721
722
723
724
725
726
727
728
729
730
731
732
733
734
735
736
737
738
739
740
741
742
743
744
745
746
747
748
749
750
751
752
753
754
755
756
757
758
759
760
761
762
763
764
765
766
767
768
769
770
771
772
773
774
775
776
777
778
779
780
781
782
783
784
785
786
787
788
789
790
791
792
793
794
795
796
797
798
799
800
801
802
803
804
805
806
807
808
809
810
811
812
813
814
815
816
817
818
819
820
821
822
823
824
825
826
827
828
829
830
831
832
833
834
835
836
837
838
839
840
841
842
843
844
845
846
847
848
849
850
851
852
853
854
855
856
857
858
859
860
861
862
863
864
865
866
867
868
869
870
871
872
873
874
875
876
877
878
879
880
881
882
883
884
885
886
887
888
889
890
891
892
893
894
895
896
897
898
899
900
901
902
903
904
905
906
907
908
909
910
911
912
913
914
915
916
917
918
919
920
921
922
923
924
925
926
927
928
929
930
931
932
933
934
935
936
937
938
939
940
941
942
943
944
945
946
947
948
949
950
951
952
953
954
955
956
957
958
959
960
961
962
963
964
965
966
967
968
969
970
971
972
973
974
975
976
977
978
979
980
981
982
983
984
985
986
987
988
989
990
991
992
993
994
995
996
997
998
999
1000

2.1.3. Pressurised Gyration

1 A schematic diagram of the gyration apparatus is shown in **Figure 1 (b)**. The rotary aluminium
2 cylindrical vessel (with a diameter of ~60 mm and a height of ~35 mm) contains 24 orifices on
3
4 its face, each having a diameter of 0.5 mm.
5
6

7
8 For the purposes of this testing, 5 ml of each polymer solution was placed in the vessel and
9
10 spun at 36, 000 rpm using 0.1 MPa applied pressure. The fibers were collected using a rod
11
12 collector placed 100 mm away from the vessel. All the spinning experiments were carried out
13
14 under ambient conditions ($22 \pm 3^\circ\text{C}$ and relative humidity of $40 \pm 3\%$). The gyration parameters
15
16 for each polymer solution are given in **Table 2**.
17
18
19
20

21 A range of applied gas pressures were trialled using PVP polymer solution to discover the
22
23 optimal pressure at which subsequent tests would be carried out. 5ml of PVP solution was spun
24
25 under at pressures ranging from 0.0 MPa to 0.3 MPa, tests were repeated 5 times at ambient
26
27 conditions. It was decided that 0.1 MPa produced fibers which has the highest yield in terms of
28
29 mass of fiber produced.
30
31
32
33
34
35
36

37 **2.2. Production of PVP Drug-loaded Fibers**

38
39 PVP was selected as the polymer to prepare drug loaded fibers. Appropriate amount of AMB
40
41 was dissolved in ethanol and added to PVP polymer solution to prepare AMB loaded PVP
42
43 fibers. Similarly, ITZ was dissolved in dichloromethane and was added to the PVP polymer
44
45 solution to prepare ITZ loaded PVP fibers. Both polymer solutions were stirred overnight with
46
47 a magnetic stirrer to form a homogenous solution of drug molecules dispersed into the polymer
48
49 solution. These polymer solutions were used to prepare 5 % w/w AMB loaded PVP fibers and
50
51
52 2.5% w/w ITZ loaded PVP fibers.
53
54
55
56
57
58

59 **2.3. Fiber Characterisation**

1
2
3
4
5
6
7
8
9
10
11
12
13
14
15
16
17
18
19
20
21
22
23
24
25
26
27
28
29
30
31
32
33
34
35
36
37
38
39
40
41
42
43
44
45
46
47
48
49
50
51
52
53
54
55
56
57
58
59
60
61
62
63
64
65

Fibers formed from both techniques were examined by Scanning Electron Microscopy (SEM). The fiber samples were gold sputter-coated (Q150R ES, Quorum Technologies) for 3 minutes preceding SEM imaging (Hitachi S-3400n). The SEM images were then surveyed using Image J software, 100 fibers were measured at random and the mean diameter was calculated. The frequency distribution of the fiber diameters was modelled using OriginPro software. Fourier Transform Infrared Spectrometry (FTIR) (Spectrum 100, PerkinElmer Inc, Beaconsfield, UK) was used to compare the chemical composition of itraconazole-loaded PVP fibers produced by electrospinning and pressurised gyration. **A summary of the average diameters of the tested polymers spun by the two techniques are presented in Table 3.**

2.4. Dissolution Studies

Dissolution tests were carried out in a controlled water bath at 37°C using PBS at pH 7.4. The tests consisted of dropping a metal sinker with 30mg of PG or ES drug-loaded fibers, encapsulated within a gelatine capsule. Drug content by weight was consistent in all samples including AMB and ITZ virgin powders. The timer started immediately following the sinking of the capsules, and 4 mL of the sample was taken and volume replaced with PBS at 37°C. The absorbance was measured at 408 nm for AMB and 254 nm for ITZ using an UV spectrometer (Jenway Instruments, 7305). All fiber samples and pure drug were tested in over a three-hour period in triplicate.

3. Results and Discussion

3.1. Fiber morphology and analysis

Fundamentally, pressurised gyration manipulates the Rayleigh-Taylor instability of the polymer solution, which explains its production mechanism. The solution is overwhelmed by

1 centrifugal force and is forced out through the apertures, reemerging as a droplet ^[20]. A surface
2 tension gradient occurs along the liquid-air interface which creates a separation of the solution
3 from the surrounding air which also focuses the jet. The surface tension gradient prompts a
4 Gibbs–Marangoni stress tangential to the liquid-gas interface, which instigates flow to the tip
5 of the polymer droplet ^[21]. The tip of the exiting droplet undergoes additional stretching and
6 thus elongates due to the pressure differential between the collection atmosphere and the drum.
7

8
9
10
11
12
13
14
15 One striking convenience of PG, is its non-electric-field driven nature thus permitting the
16 spinning of an almost-limitless number of polymers. This is also in contrast to ES, where the
17 electric field limits the choice of polymer. ES has been widely recognised as a simple, versatile
18 and facile method for fabrication of polymeric fibers with a wide range of uses including drug
19 delivery. Pressure-driven nanofiber production methods such as pressurised gyration offer a
20 compelling alternative to electric-field driven technologies such as electrospinning. This comes
21 with the ability to spin charge-absent polymers and potentially improve production yield.
22 However, a comparison in the fiber morphology, accessibility and final product performance
23 (drug delivery) has yet to be completed.
24
25
26
27
28
29
30
31
32
33
34
35
36
37

38 The magnitude of applied gas pressure had a consequence on the production yield of pressurised
39 gyration PVP fibers. **Figure 2** shows the effect of gas pressure on the mass of fibers produced
40 by pressurised gyration. We can see from the graph that the effective yield reduces as gas
41 pressure increases. During the spin-up time of the motor in which the motor accelerates to
42 maximum velocity, higher pressures cause a scattering effect on the polymer solution which
43 causes the solvent to be lost through the orifices. At these lower rotation speeds, the centrifugal
44 force does not surpass the surface tension of the polymer solution and thus a polymer jet is not
45 formed. It can be observed during initial rotation that higher pressures result in more solvent
46 being displaced on the collection surfaces. Higher pressure gas streams have higher kinetic
47 energy thus increasing its velocity. The high velocity of the gas creates a driving force for the
48
49
50
51
52
53
54
55
56
57
58
59
60
61
62
63
64
65

1 acceleration of the solvent out through the orifices [22]. At 0 MPa pressure, the average yield
2 was greatest at 81mg (± 4). No overlap in the error bars and the presence of linear regression
3
4 with a R^2 value of 0.99 suggests that yield in terms of fiber mass decreases with increasing gas
5
6 pressure. This inherent disadvantage can however be overcome by applying the gas pressure
7
8 after critical rotation speed has been reached. The delay in applying the gas pressure will ensure
9
10 that solution and solvent are not forced out of the orifices which will lead in maximum yields
11
12 being obtained. Thus, most experiments in this work were carried out at 0.1 MPa to minimise
13
14 human error in judging when critical rotation speeds were met.
15
16
17
18
19

20 **3.2. Fiber Characterisation**

21
22
23

24 Surface topography of the PVP fibers formed via ES and PG (**Figure 3**) both showed a smooth
25
26 and pore-less surface. Fibers produced by ES exhibited a cross-woven profile with overlapping
27
28 fibers, due to the agitated motion of the whipping instability onto the grounded collector [23].
29
30 PG fibers were found to be more aligned due to the unidirectional rotation of the drum and
31
32 outward force of the applied gas pressure [24]. Cross-woven fibers could however attribute to a
33
34 superior drug-release profile as there is increased steric hindrance of the drug molecules in their
35
36 amorphous state [25]. The fiber diameter distribution of ES fibers demonstrated a smaller
37
38 variation, proving that ES created more uniform fibers with a smaller diameter. ES provided
39
40 greater control over fiber diameter due to having more processing parameters, capable of fine-
41
42 tuning fiber diameter, however in more recent processes like pressure-coupled infusion
43
44 gyration, this limitation can be overcome [26]. In pressure-driven fiber formation, the minimum
45
46 achievable diameter is limited by the orifice area and the compactability of the polymer [27].
47
48 Increasing the rotational speed would result in a higher centrifugal force which could result in
49
50 finer diameter fibers for PG [9].
51
52
53
54
55
56
57
58

59 Centrifugal dispersion affects fiber diameter, uniformity and alignment [28]. At higher rotational
60
61 speeds, the centrifugal force overcomes the surface tension of the solution, increasing fiber
62
63
64
65

1 uniformity. From the SEM images, PG-formed PVDF fibers displayed a more aligned
2 configuration especially when compared to ES fibers (**Figure 4**), this is predominantly due to
3
4 unidirectional high speed rotation of the pressurised gyration drum. Fiber uniformity was
5
6 noticeably greater with PG fibers; this is possibly due to the rotational speed being matched
7
8 with the surface tension of the 30% w/w solution ($28.1 \pm 0.5 \text{ mNm}^{-1}$). The bending instability
9
10 of the polymer jet is corrected for by the centrifugal force, in ES the instability sees no
11
12 modification and fibers are deposited as a cross-woven mat ^[29]. Fiber diameters were also
13
14 observed to be significantly finer with PG with a smaller spread about the mean. This further
15
16 supports that an optimal rotational speed was created for the polymer system in PG. The ES
17
18 PVDF solution required a flow rate of 50 $\mu\text{L}/\text{min}$ and a voltage of 18.0 kV, indicating a higher
19
20 surface tension than PVP ($21.6 \pm 0.9 \text{ mNm}^{-1}$) which had to be overcome with a higher voltage
21
22 ^[30]. Physical characteristics of the polymer solvents used are summarised in **Table 4**.
23
24
25
26
27
28
29

30 The occurrence of “bead-on-string” morphology has been a point of interest in electrospinning
31
32 studies, with many attributing this behaviour to instabilities resulting from low charge density
33
34 or surface tension of the solution (PMMA surface tension: $26.8 \pm 0.4 \text{ mNm}^{-1}$) ^[31-33]. ES PMMA
35
36 fibers showed a beaded morphology whilst PG did not (**Figure 5**). This interesting outcome
37
38 could be the result of having a low charge density in ES, whilst centrifugal-lead spinning in PG
39
40 does not require the exploitation of charge. Both PG and ES produced fibers with a porous
41
42 topography. Formation of pores requires a highly volatile solvent such as chloroform which
43
44 creates a temperature drop resulting in formation of water droplets, these droplets then
45
46 evaporate forming pores ^[10], The average pore size was 390 nm (± 68) for ES fibres and 70 nm
47
48 (± 18) for PG fibres. Pores found on ES fibers had a significantly larger average diameter, which
49
50 could be explained by the necessary use of high flow rate to overcome solution stagnation ^[34].
51
52 Average fiber diameter of PG fibers were again notably smaller and less dispersed than ES
53
54 fibers. This shows that PG is capable of producing finer diameter fibers on some polymer
55
56
57
58
59
60
61
62
63
64
65

1 systems that would otherwise be very difficult to spin with ES. It must be noted that PMMA
2 fiber production were very high in PG and in ES. However, prolonged electrospinning was not
3 possible because the solution would eventually clog the needle causing blockages.
4
5
6

7
8 PNIPAm ES fibers exhibited an average fiber diameter of 3.0 μm (± 0.5), displaying high
9 uniformity. PG fibers produced a larger average fiber diameter at 6.3 μm (± 3.6) with a high
10 spread of diameters as shown in **Figure 6**. A high flow rate typically produces electrospun
11 fibers with a thicker diameter owing to the shorter drying time of the solvent before reaching
12 the collector and the reduced stretching forces ^[35]. However even at a high flow rate of 150
13 $\mu\text{L}/\text{min}$, ES PNIPAm fibers produced smaller diameter fibers with a tighter size distribution
14 compared to PG fibers. At high viscosities in PG, fiber stretching becomes more difficult and
15 as a consequence, thicker fibers are produced with a wider diameter distribution ^[36]. Although
16 not a particularly high molecular weight polymer (300,000 g mol^{-1}), PNIPAm has a high
17 viscosity (654.1 $\text{mPa}\cdot\text{s}$) due to its polar ester group promoting stronger interactions in its inter-
18 chains ^[37]. Electrospun PNIPAm fibers displayed a very uniform diameter distribution with
19 very little spread. The surface was smooth in fibers produced by both technologies. It must be
20 noted that there was difficulty with electrospinning the PNIPAm solution due to its high
21 viscosity. A large flow rate was required to overcome solution stagnation and tube blocking.
22 Even at a high flow rate (150 $\mu\text{L}/\text{min}$) the solution would not allow prolonged spinning
23 sessions. In comparing simplicity and processability, pressurised gyration did not pose any
24 difficulties when spinning PNIPAm, providing feasibility which was not shown by
25 electrospinning.
26
27
28
29
30
31
32
33
34
35
36
37
38
39
40
41
42
43
44
45
46
47
48
49
50

51
52 Comparing pressure-driven fiber forming techniques with electric field driven techniques, there
53 are notable differences in the production mechanism. One key element contributing to fiber
54 thinning is solvent evaporation ^[38]. Pressurised gyration is capable of forming finer diameter
55 fibers such as in the case of PMMA and PINIPAm. When dimethylformamide, acetone and
56
57
58
59
60
61
62
63
64
65

1 chloroform were used as solvents, they produced lower diameter fibers using pressurised
2 gyration than electrospinning. The high volatility of these solvents ensures rapid evaporation
3
4 from the emerging polymer jets. The rotation of the spinning vessel also accelerates solvent
5 evaporation by increasing the kinetic energy of the solvents in the emerging droplets.
6
7

8
9
10 Electrospinning produced fibers with finer diameters for PVP and PNIPAm, coincidentally both
11 polymers were dissolved in ethanol. The principle of electro spray Ionisation (ESI) can be used
12 to explain the ionisation of the ethanol in a polymer solution. Given sufficient polymer chain
13 entanglement, the polymer is not atomised. However, the solvent undergoes ionisation in the
14 same way as it would under ESI. Solvent evaporation occurs when the droplets traverses
15 between the opening of the nozzle and the open environment ^[39]. As solvent evaporation ensues,
16 the size of the droplets decreases until reaching the Rayleigh limit. Coulomb fission occurs
17 when the droplets reach the Rayleigh limit and are unable to withstand the Coulomb force of
18 repulsion ^[40]. Initial droplets disintegrate creating smaller “offspring” droplets. Coulomb
19 fission and solvent evaporation occur repeatedly generating increasingly smaller droplets which
20 finally become charged nano-droplets from which the gas-phase charged molecules form ^[41].
21
22 Due to the presence of an electric field in electrospinning, solvent evaporation rates are
23 accelerated by Coulomb fission. Ethanol is readily atomised which potentially explains the
24 difference in fiber diameter between ES and PG, as the atomisation increases solvent
25 evaporation rate in electrospinning but not pressurised gyration.
26
27
28
29
30
31
32
33
34
35
36
37
38
39
40
41
42
43
44
45
46

47 **3.3. Drug-loaded Fibers and dissolution studies**

48
49 Poorly water soluble drugs ITZ (water solubility 1-4 ng/mL) and AMB (water solubility 0.08
50 mg/mL) were selected to prepare drug loaded fibers ^[42, 43]. AMB-loaded and ITZ-loaded PVP
51 fibers were successfully produced using both ES and PG. SEM analysis revealed all the fibers
52 were cylindrical in shape, with smooth surfaces and no visible particles. This indicates that
53 AMB and ITZ were successfully encapsulated homogenously within the polymeric fibers. The
54
55
56
57
58
59
60
61
62
63
64
65

1 SEM images of the drug loaded fiber are given in **Figure 7.** and fiber diameters are tabulated
2 in **Table 3.** Smaller fiber diameters are highly desirable in drug delivery applications, as this
3
4 drastically improves their contact surface area: volume ratio, thus also improving the drug
5
6 dissolution rate. Electrospinning produced drug loaded PVP fibers with finer diameters as
7
8 compared with pressurised gyration.
9
10

11
12 The drug dissolution profile (**Figure 8**) evidently illustrates that drug-loaded PVP fibers
13
14 significantly improve the dissolution of AMB and ITZ. The dissolution enhancement of AMB
15
16 and ITZ can be attributed to several factors. Essential factors for dissolution rate improvement
17
18 include amorphisation, particle size reduction, improved dispersibility and wettability^[44]. It can
19
20 be eluded from the dissolution data of drug-loaded fibers that improvement in dissolution is
21
22 ascribed to the increased wettability and dispersibility that PVP provides. The mixing of AMB
23
24 and ITZ with the hydrophilic PVP resulted in superior wetting, this increased the contact surface
25
26 area for dissolution as it reduced the interfacial tension between the hydrophobic AMB and ITZ
27
28 and the dissolution media^[45]. It is expected that the drug molecules were uniformly distributed
29
30 within the polymer in a highly dispersed state. When in contact with the dissolution media, the
31
32 hydrophilic PVP readily dissolved and this resulted in the precipitation of the embedded drug
33
34 into fine colloidal particles. The absence of drug molecule aggregation due to steric hindrance
35
36 of the polymer chains and the amorphisation of the drug could have also attributed to the
37
38 enhanced dissolution profile of the PG and ES drug-loaded fibers^[46].
39
40
41
42
43
44
45
46

47
48 There is an observable difference between the dissolution rates of the PG fibers compared with
49
50 the ES fibers. The distribution of AMB and ITZ drug molecules within the polymer chain would
51
52 have been influenced by the electric field of electrospinning, where the pressure and centrifugal
53
54 force of pressurised gyration would not have. Alternatively, the cross-woven conformation of
55
56 ES fibers may have reduced the available surface area via a “barrier effect” of the interlaced
57
58 fiber branches. **Via the close overlapping of fiber branches, effective surface area is reduced as**
59
60
61
62
63
64
65

1 the fibers aggregate creating a “barrier” of fibers which act as larger diameter branches. A
2 reduced surface area yields fewer electrostatic interactions between the polar molecules of the
3
4 dissolution media and the polymer surface [47]. PG fibers consistently displayed absence of
5
6 release within the first 10 minutes, this could be due to the dispersion of drug molecules within
7
8
9 the centre of the fibers due to the rotation of the gyration vessel. Structure of the fibers produced
10
11 by the two techniques seem to play a role in the release kinetics. ES fibers were finer in diameter
12
13 and also revealed earlier release when these came in contact with the dissolution media. The
14
15 finer diameter afforded for greater surface area as the hydrogen bonds of the PVP chain were
16
17 being broken. PG fibers had a slightly larger diameter which could explain the delay in drug
18
19
20
21
22 release.

23
24
25 The FTIR absorption spectra of the itraconazole-loaded PVP fibers are shown in **Figure 9**. The
26
27 peak at 3430 cm^{-1} corresponds to the O-H stretching vibration of PVP, peak at 1018 cm^{-1}
28
29 matches the C-N vibrations [48]. Characteristic peaks observed at $2824 - 3128\text{ cm}^{-1}$ were due to
30
31 C-H vibrations, showing itraconazole was present [49]. Peaks at 1660 cm^{-1} show the C=O
32
33 stretching vibrations of PVP. The two fibers types show superimposability suggesting they have
34
35 almost identical chemical properties. The FTIR spectrum corroborated that the itraconazole-
36
37 loaded PVP fibers produced by ES and PG contained itraconazole. Characteristic peaks at 2824
38
39
40
41
42
43
44
45
46
47
48
49
50
51
52
53
54
55
56
57
58
59
60
61
62
63
64
65
The FTIR spectrum thus demonstrates that the ITZ fibers produced by ES and PG do not
differ in their chemical makeup, as expected. Any differences in the drug-release profile is more
likely due to structural differences in the fibers such as the aforementioned “cross woven”

1
2
3
4
5
6
7
8
9
10
11
12
13
14
15
16
17
18
19
20
21
22
23
24
25
26
27
28
29
30
31
32
33
34
35
36
37
38
39
40
41
42
43
44
45
46
47
48
49
50
51
52
53
54
55
56
57
58
59
60
61
62
63
64
65

conformation of fibers produced by pressurised gyration and the differences in fiber morphology,

When comparing the drug release profiles between AMB and ITZ, it can be seen that there is a general pattern. Both AMB and ITZ drug loaded PVP fibers showed extensive increase in dissolution when compared to the dissolution of drug powder. The increase in dissolution rate of AMB drug compared with ITZ drug is merely due to its greater solubility. Fibers spun by PG displayed consistent maximum release whilst ES fibers showed inconsistent release. Pressurised gyration fibers are thus able to release the active pharmaceutical ingredient in a more precise and predictable manner which is highly desired in drug delivery. Itraconazole loaded fibers produced by PG show accelerated release in contrast to a slightly delayed maximum release with electrospun fibers. The difference in release profile for itraconazole fibers is likely due to the difference in fiber morphology. Furthermore, it can be seen that PG drug loaded fibers do not express any release within the first 10 minutes of testing, whereas ITZ ES fibers show release within the first 5 minutes. Slight differences between the dissolution profile of AMB and ITZ loaded fibers can be ascribed to PVP's tendency to bind differently to different drugs via hydrogen bonding, where the two drugs differed in their chemical structure. The difference in drug loading between AMB (5%) and ITZ (2.5%) fibers showed a predictable shift in the maximum release times with PG fibers releasing at 55 minutes for AMB and 30 minutes for ITZ. The drug release profile can thus be tailored by multiple parameters. The working parameters of electrospinning and pressurised gyration allow configuration of drug loaded fibers that can vary in fiber diameter, structure and drug to polymer ratio. Pressurised gyration alongside electrospinning has proven to be a dependable method of producing fibers for drug delivery, pressurised gyration allows for additional reliability in controlled drug delivery of poorly water-soluble drugs.

4. Conclusions

Several types of polymeric fibers were prepared with two different fiber making techniques: electrospinning and pressurised gyration. PVP, PVDF, PMMA and PINIPAm were selected as the polymers. Pressurised gyration produced finer diameter fibers with polyvinylidene fluoride and Poly(methyl methacrylate) as compared with electrospinning. On the other hand, fiber diameter of gyrospun poly(*N*-isopropylacrylamide) was larger than electrospun fibers and fiber diameter of both electrospun and gyrospun Poly(vinylpyrrolidone) fibers have roughly similar fiber diameters. Needle clogging and polymer solution flowing difficulties were observed during electrospinning. Such difficulties were not observed with pressurised gyration and fiber production rate was higher in this technique compare to electrospinning. Amphotericin B and itraconazole loaded PVP fibers were prepared using both techniques. In-vitro dissolution studies showed a more rapid release with electrospun fibers than gyrospun fibers at the beginning, for 15 minutes. Gyrospun fibers showed accelerated dissolution following 15 minutes and were able to reach 100% release due to their structure and morphology. Both ES and PG fibers are suitable for improving the dissolution of poorly water soluble drugs, pressurised gyration offers promising potential in producing controlled and specific-release pharmacokinetics.

References

- [1] M. Gagliardi, "Global Markets and Technologies for Nanofibers", USA, 2016.
- [2] M. C. Wang, G. D. Pins, F. H. Silver, *Biomaterials* **1994**, *15*, 507.
- [3] P. X. Ma, R. Zhang, *Journal of Biomedical Materials Research* **1999**, *46*, 60.
- [4] G. M. Whitesides, B. Grzybowski, *Science* **2002**, *295*, 2418.
- [5] Z.-M. Huang, Y. Z. Zhang, M. Kotaki, S. Ramakrishna, *Composites Science and Technology* **2003**, *63*, 2223.
- [6] Y. Márquez, L. Franco, P. Turon, L. J. del Valle, J. Puiggali, *Macromolecular Materials and Engineering* **2017**, 1700401.
- [7] L. Persano, A. Camposeo, C. Tekmen, D. Pisignano, *Macromolecular Materials and Engineering* **2013**, *298*, 504.
- [8] X. Hong, S. Mahalingam, M. Edirisinghe, *Macromolecular Materials and Engineering* **2017**, *302*, 1600564.
- [9] Y. Lu, Y. Li, S. Zhang, G. Xu, K. Fu, H. Lee, X. Zhang, *European Polymer Journal* **2013**, *49*, 3834.
- [10] U. Illangakoon, S. Mahalingam, R. Matharu, M. Edirisinghe, *Polymers* **2017**, *9*, 508.
- [11] J. L. Daristotle, A. M. Behrens, A. D. Sandler, P. Kofinas, *ACS Applied Materials & Interfaces* **2016**, *8*, 34951.
- [12] W. Reppe, *Angewandte Chemie* **1953**, *65*, 577.
- [13] F. Haaf, A. Sanner, F. Straub, *Polymer Journal* **1985**, *17*, 143.
- [14] T. R. Bates, *Journal of Pharmacy and Pharmacology* **1969**, *21*, 710.
- [15] L. P. Zhu, J. Z. Yu, Y. Y. Xu, Z. Y. Xi, B. K. Zhu, *Colloids and surfaces. B, Biointerfaces* **2009**, *69*, 152.
- [16] G. Lewis, *Journal of Biomedical Materials Research* **1997**, *38*, 155.
- [17] J. Zhang, N. A. Peppas, *Macromolecules* **2000**, *33*, 102.
- [18] M. Chen, M. Dong, R. Havelund, V. R. Regina, R. L. Meyer, F. Besenbacher, P. Kingshott, *Chemistry of Materials* **2010**, *22*, 4214.
- [19] H. Friedrich, B. Fussnegger, K. Kolter, R. Bodmeier, *European Journal of Pharmaceutics and Biopharmaceutics* **2006**, *62*, 171.

- 1 [20] S. Mahalingam, B. T. Raimi-Abraham, D. Q. M. Craig, M. Edirisinghe, *Chemical*
2 *Engineering Journal* **2015**, 280, 344.
- 3 [21] X. Xu, J. Luo, *Applied Physics Letters* **2007**, 91, 124102.
- 4
5 [22] E. S. Medeiros, G. M. Glenn, A. P. Klamczynski, W. J. Orts, L. H. C. Mattoso, *Journal of*
6 *Applied Polymer Science* **2009**, 113, 2322.
- 7
8 [23] R. Jalili, M. Morshed, S. A. H. Ravandi, *Journal of Applied Polymer Science* **2006**, 101,
9 4350.
- 10
11 [24] J. Pal, S. Singh, S. Sharma, R. Kulshreshtha, B. Nandan, R. K. Srivastava, *Materials*
12 *Letters* **2016**, 167, 288.
- 13
14 [25] B. Rambali, G. Verreck, L. Baert, D. L. Massart, *Drug development and Industrial*
15 *Pharmacy* **2003**, 29, 641.
- 16
17 [26] J. Du, S. Shintay, X. Zhang, *Journal of Polymer Science Part B: Polymer Physics* **2008**,
18 46, 1611.
- 19
20 [27] J. Dudowicz, K. F. Freed, *Macromolecules* **1991**, 5112.
- 21
22 [28] D. Edmondson, A. Cooper, S. Jana, D. Wood, M. Zhang, *Journal of Materials Chemistry*
23 **2012**, 22, 18646.
- 24
25 [29] F. Dabirian, S. A. Hosseini Ravandi, A. R. Pishavar, R. A. Abuzade, *Journal of*
26 *Electrostatics* **2011**, 69, 540.
- 27
28 [30] X. Zong, K. Kim, D. Fang, S. Ran, B. S. Hsiao, B. Chu, *Polymer* **2002**, 43, 4403.
- 29
30 [31] Y. Liu, J.-H. He, J.-y. Yu, H.-m. Zeng, *Polymer International* **2008**, 57, 632.
- 31
32 [32] W. Zuo, M. Zhu, W. Yang, H. Yu, Y. Chen, Y. Zhang, *Polymer Engineering & Science*
33 **2005**, 45, 704.
- 34
35 [33] T. Lin, H. Wang, H. Wang, X. Wang, "The charge effect of cationic surfactants on the
36 *elimination of fibre beads in the electrospinning of polystyrene*", 2004, p. 1375.
- 37
38 [34] J. Rnjak-Kovacina, S. G. Wise, Z. Li, P. K. Maitz, C. J. Young, Y. Wang, A. S. Weiss,
39 *Biomaterials* **2011**, 32, 6729.
- 40
41 [35] C. J. Buchko, L. C. Chen, Y. Shen, D. C. Martin, *Polymer* **1999**, 40, 7397.
- 42
43 [36] J. E. Oliveira, L. H. C. Mattoso, W. J. Orts, E. S. Medeiros, *Advances in Materials Science*
44 *and Engineering* **2013**, 2013, 14.
- 45
46 [37] D. E. Bergbreiter, B. L. Case, Y.-S. Liu, J. W. Caraway, *Macromolecules* **1998**, 31, 6053.
- 47
48 [38] Y. Dzenis, *Science* **2004**, 304, 1917.
- 49
50 [39] S. Banerjee, S. Mazumdar, *International Journal of Analytical Chemistry* **2012**, 2012, 1.
- 51
52
53
54
55
56
57
58
59
60
61
62
63
64
65

[40] P. Kebarle, L. Tang, *Analytical Chemistry* **1993**, 65, 972A.

[41] J. V. Iribarne, B. A. Thomson, *The Journal of Chemical Physics* **1976**, 64, 2287.

[42] J. C. DiNunzio, C. Brough, D. A. Miller, R. O. Williams, J. W. McGinity, *Journal of Pharmaceutical Sciences* **2010**, 99, 1239.

[43] R. Mannhold, G. I. Poda, C. Ostermann, I. V. Tetko, *J Pharm Sci* **2009**, 98, 861.

[44] J. L. Ford, *Pharmaceutica acta Helvetiae* **1986**, 61, 69.

[45] A. Modi, P. Tayade, *AAPS PharmSciTech* **2006**, 7, E87.

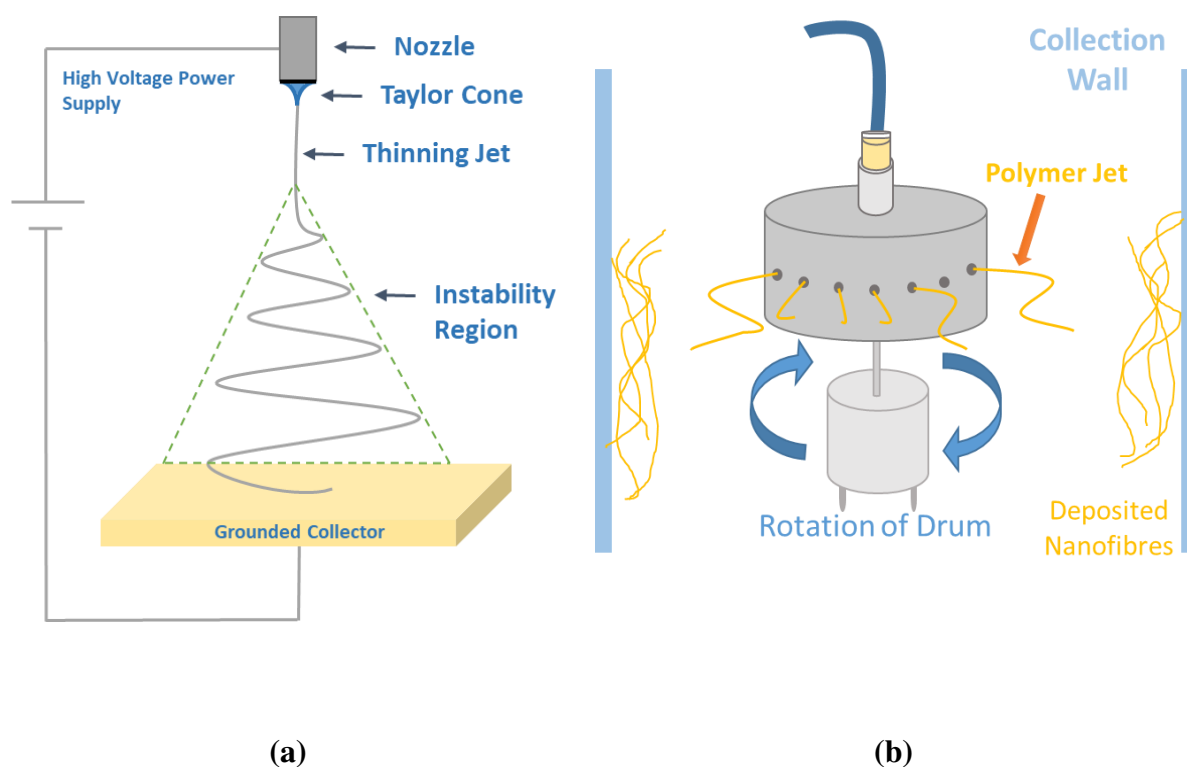
[46] P. Mura, A. Manderioli, G. Bramanti, L. Ceccarelli, *Drug Development and Industrial Pharmacy* **1996**, 22, 909.

[47] M. L. Sanchez, M. A. Aguilar, F. J. O. delValle, *Journal of Computational Chemistry* **1997**, 18, 313.

[48] L. S. Taylor, G. Zograf, *Pharmaceutical Research* **1997**, 14, 1691.

[49] K. Malarvizhi, D. Ramya, A. Raymond, D. B. N. V. Hari, "Engineered Nanoparticle Aerosol Foam Formulation for Skin Diseases", 2014, p. 109.

[50] T. Tao, Y. Zhao, J. Wu, B. Zhou, *International Journal of Pharmaceutics* **2009**, 367, 109.



1
2
3
4
5
6
7
8
9
10
11
12
13
14
15
16
17
18
19
20
21
22
23
24
25
26
27
28
29
30
31
32
33
34
35
36
37
38
39
40
41
42
43
44
45
46
47
48
49
50
51
52
53
54
55
56
57
58
59
60
61
62
63
64
65

Figure 1. (Schematic diagrams illustrating (a) electrospinning (b) pressurised gyration setups used)

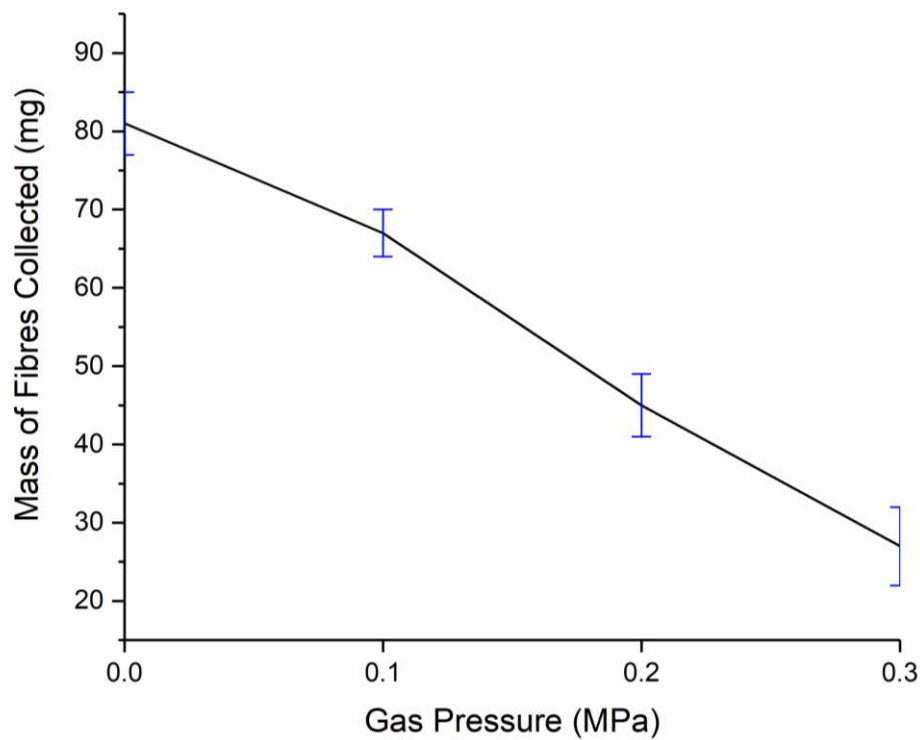
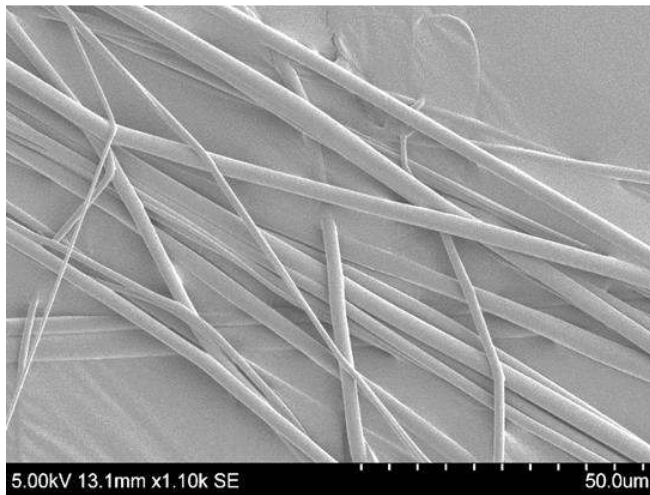
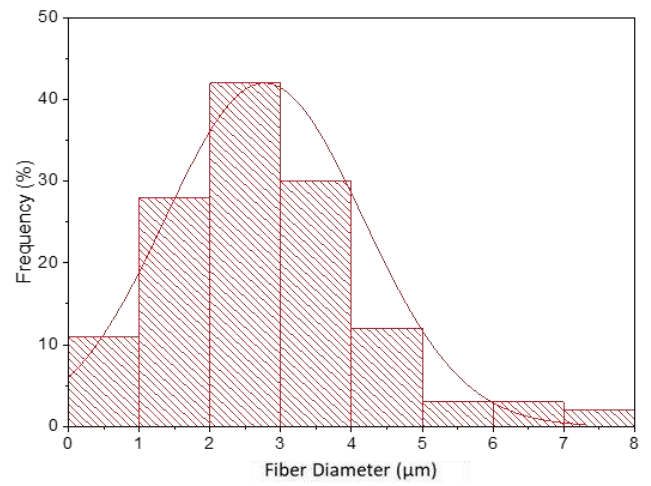


Figure 2. Shows the effect of increasing gas pressure on the of fibre yield, spun for 15 seconds at a speed of 36,00 rpm. The standard deviation of the repeated tests is represented by error bars (n = 5).

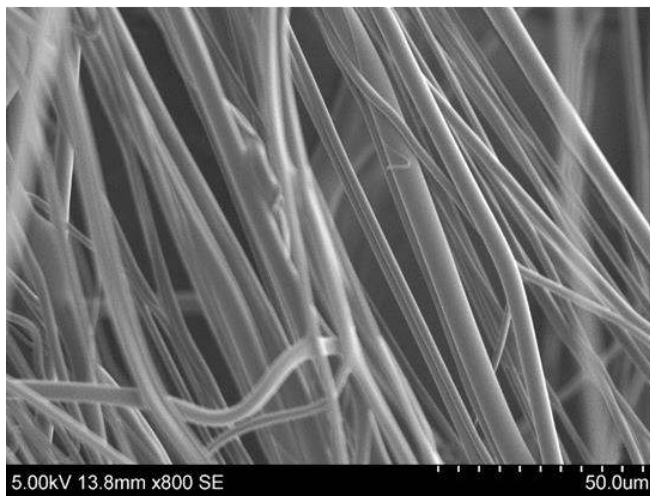


16
17
18
19
20
21
22
23
24
25
26
27
28
29
30
31
32
33
34
35
36

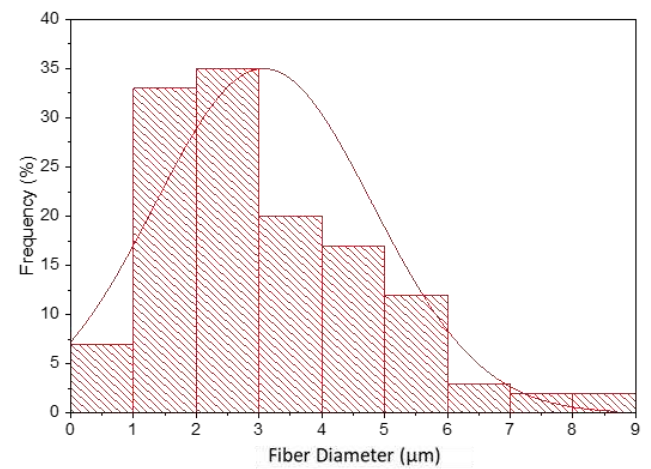
a)



b)



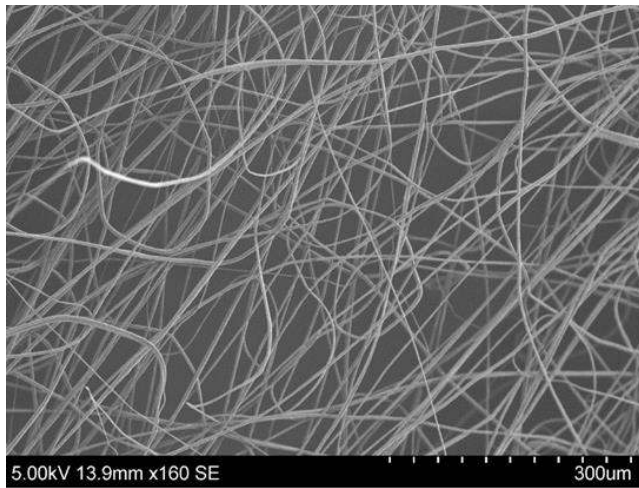
c)



d)

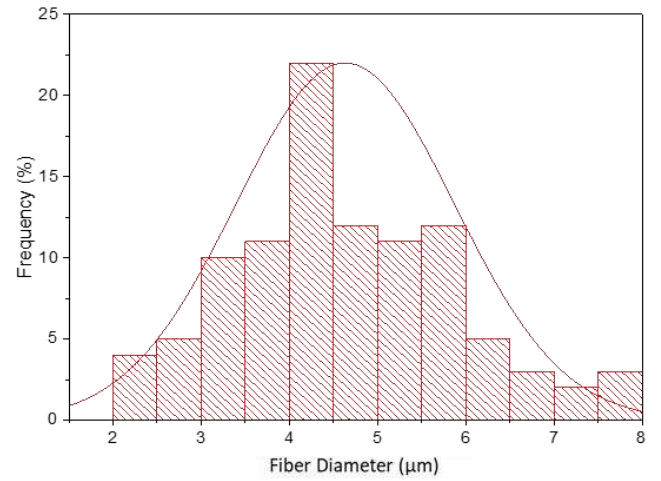
37
38
39
40
41
42
43
44
45
46
47
48
49
50
51
52
53
54
55
56
57
58
59
60
61
62
63
64
65

Figure 3. SEM images and fibre diameter distribution of PVP fibres prepared by electrospinning (a, b) and pressurised gyration (c, d).

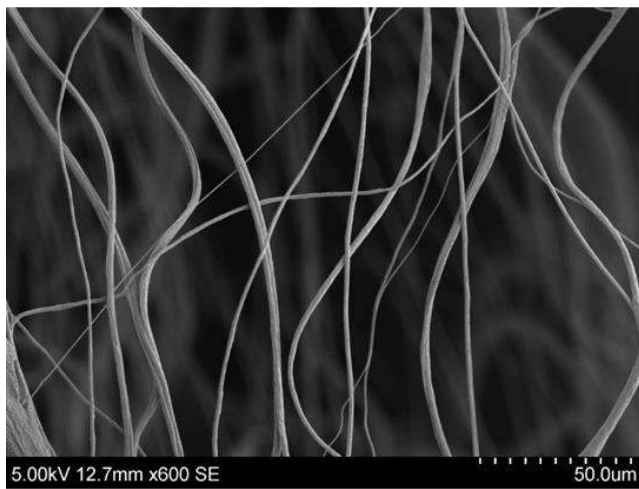


16
17
18
19
20
21
22
23
24
25
26
27
28
29
30
31
32
33
34
35
36

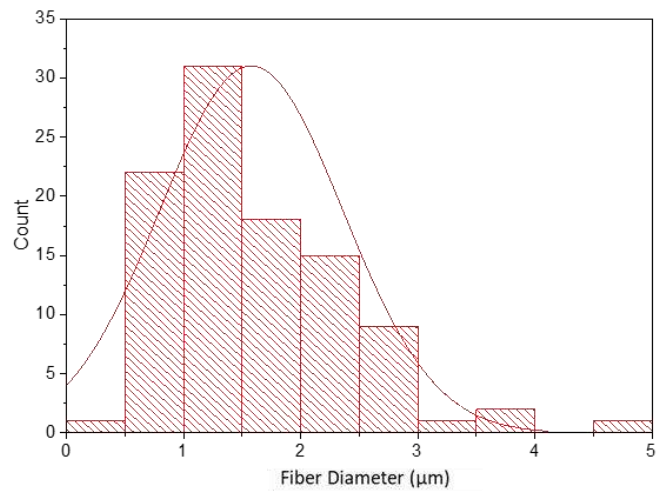
a)



b)



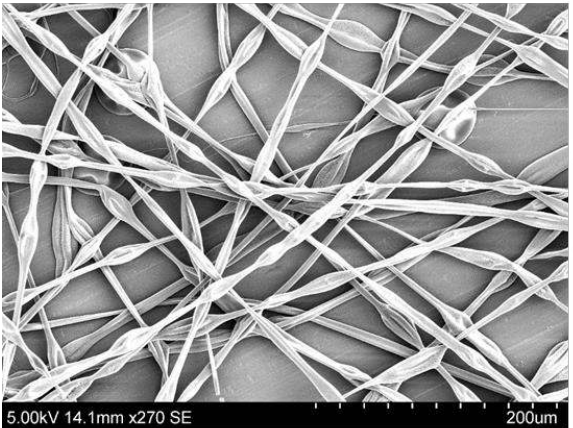
c)



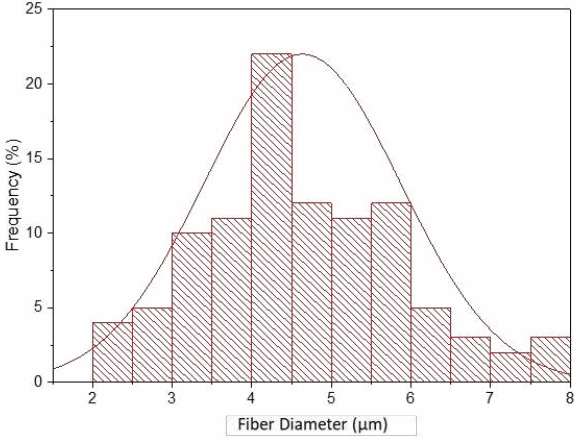
d)

Figure 4. SEM images and fibre diameter distribution of PVDF fibres prepared by (a,b) electrospinning and (c,d) pressurised gyration.

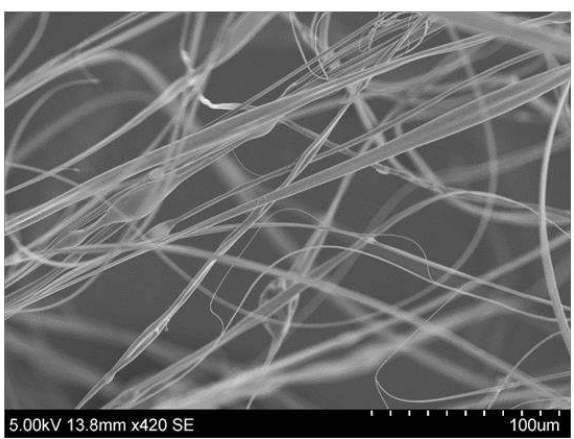
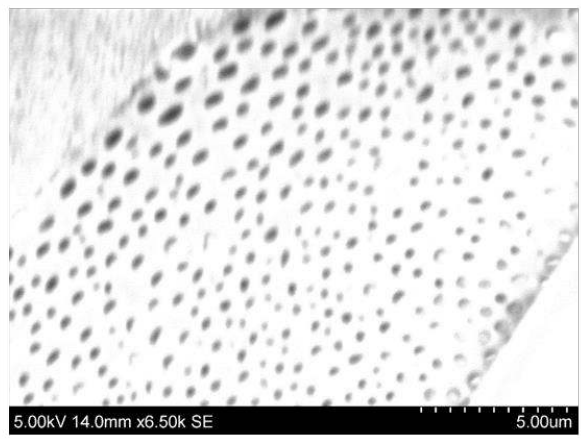
1
2
3
4
5
6
7
8
9
10
11
12
13
14
15
16
17
18
19
20
21
22
23
24
25
26
27
28
29
30
31
32
33
34
35
36
37
38
39
40
41
42
43
44
45
46
47
48
49
50
51
52
53
54
55
56
57
58
59
60
61
62
63
64
65



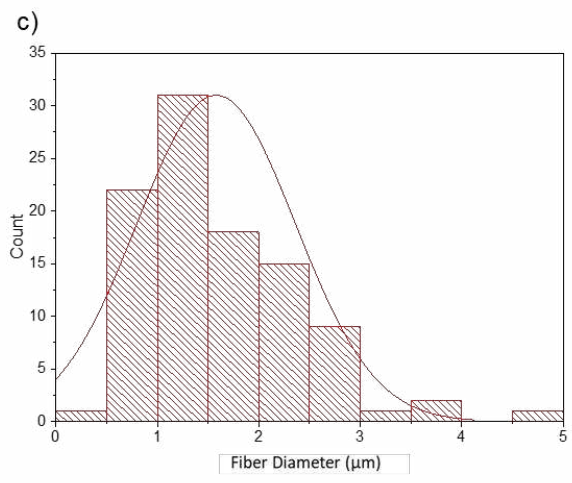
a)



b)



d)



e)

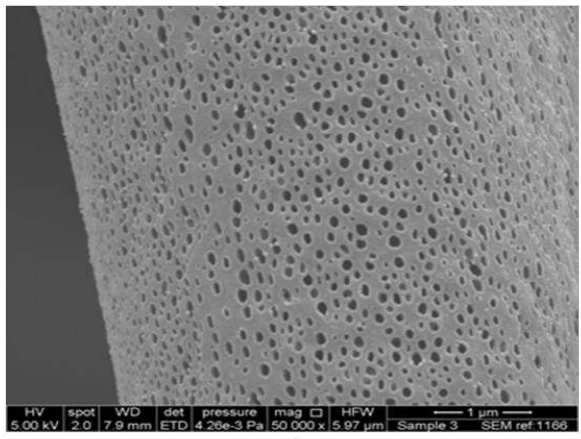
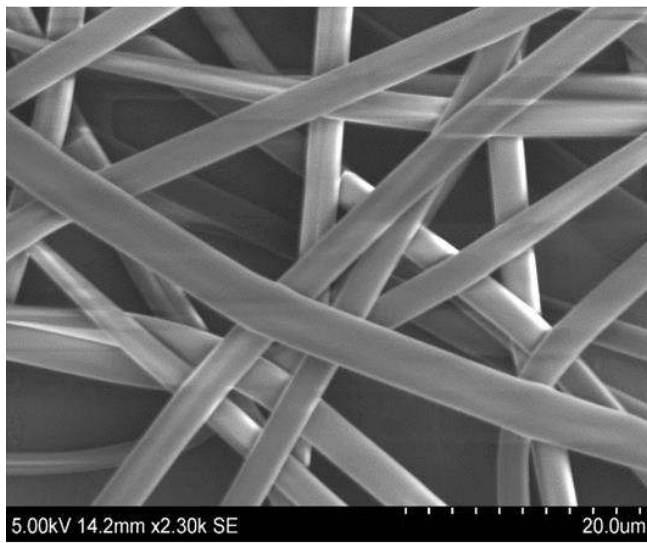
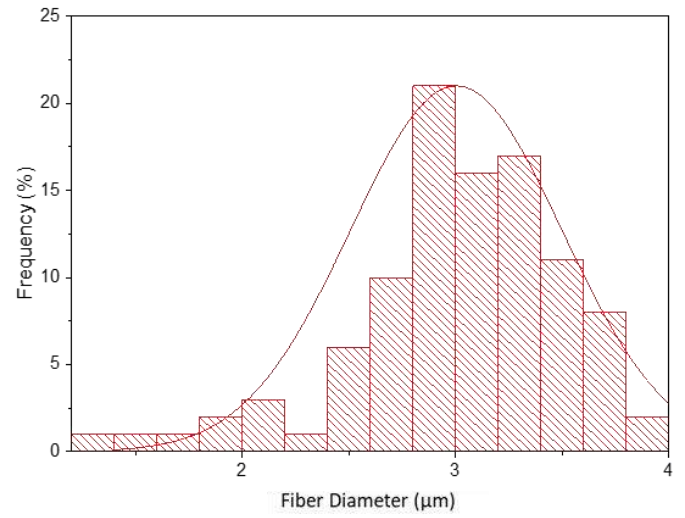


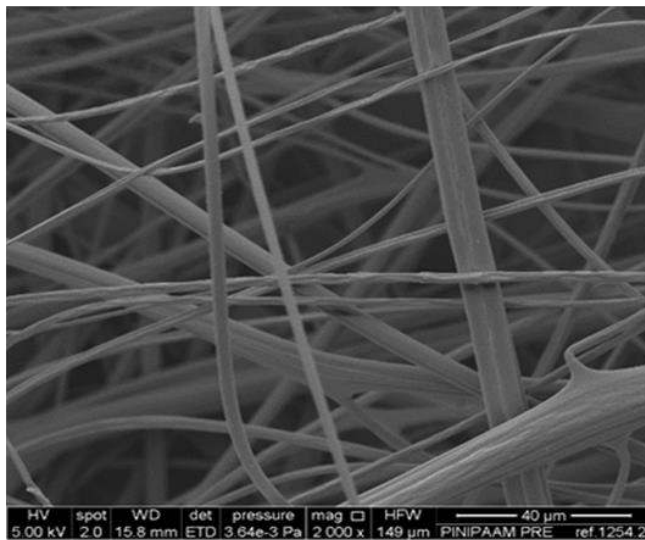
Figure 5. SEM images and fiber diameter distribution of PMMA fibres prepared by electrospinning (a, b, c) and pressurised gyration (d, e, f).



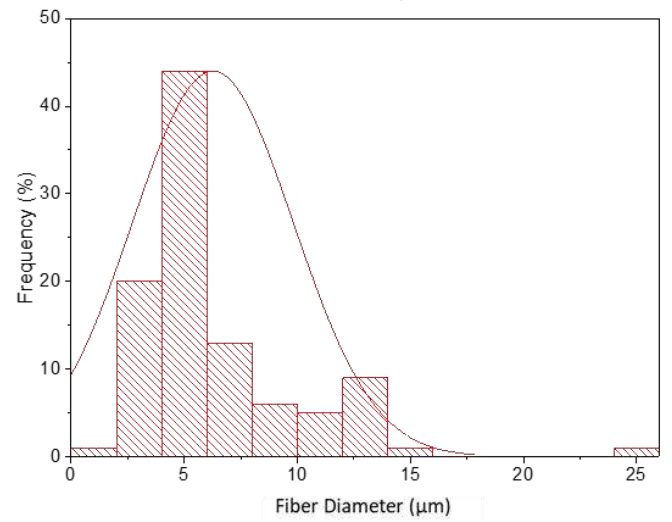
a)



b)

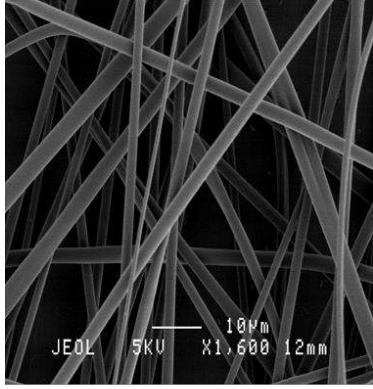


c)

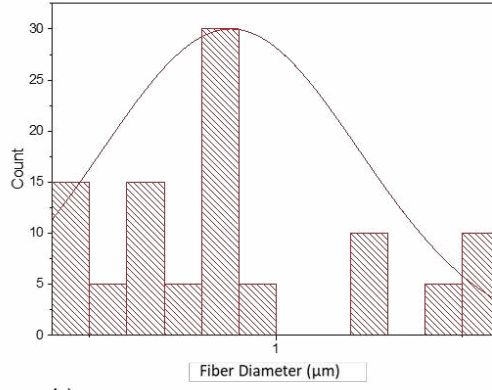


d)

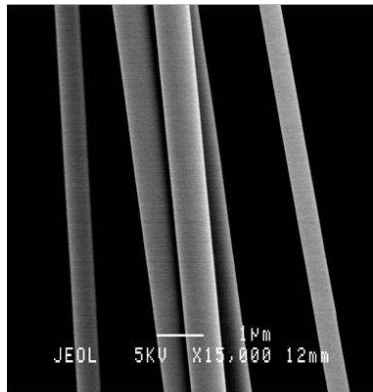
Figure 6. SEM images and fiber diameter distribution of PINIPAM fibres prepared by electrospinning (a, b) and pressurised gyration (c, d).



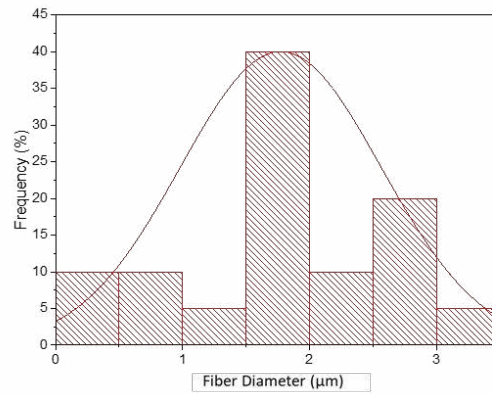
a)



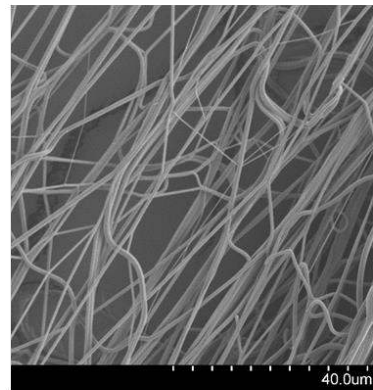
b)



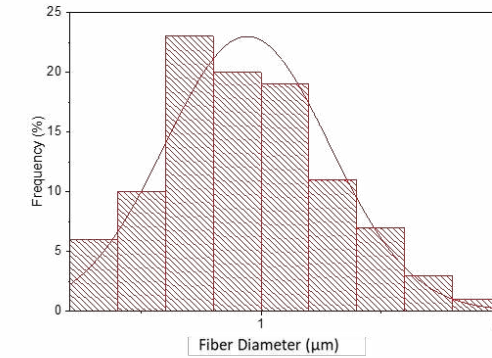
c)



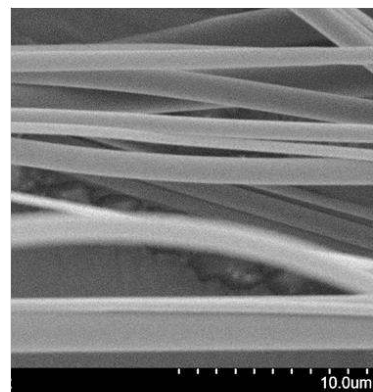
d)



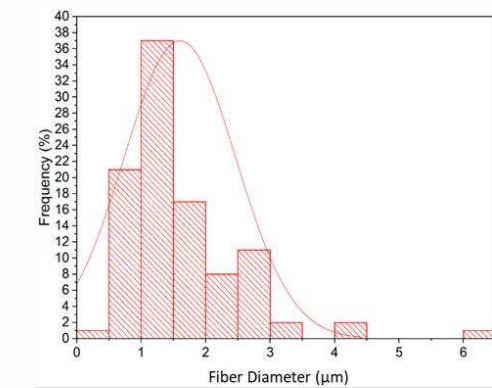
e)



f)



g)



h)

1
2
3
4
5
6
7
8
9
10
11
12
13
14
15
16
17
18
19
20
21
22
23
24
25
26
27
28
29
30
31
32
33
34
35
36
37
38
39
40
41
42
43
44
45
46
47
48
49
50
51
52
53
54
55
56
57
58
59
60
61
62
63
64
65

1
2
3
4
5
6
7
8
9
10
11
12
13
14
15
16
17
18
19
20
21
22
23
24
25
26
27
28
29
30
31
32
33
34
35
36
37
38
39
40
41
42
43
44
45
46
47
48
49
50
51
52
53
54
55
56
57
58
59
60
61
62
63
64
65

Figure 7. SEM images and fibre diameter distribution of: Amphotericin B loaded PVP fibres prepared by electrospinning (a) and pressurised gyration (c), Itraconazole loaded PVP fibres produced by (e) electrospinning and (g) pressurised gyration. Figures (b,d,f,h) show the fibre diameter distribution for the corresponding fibre type.

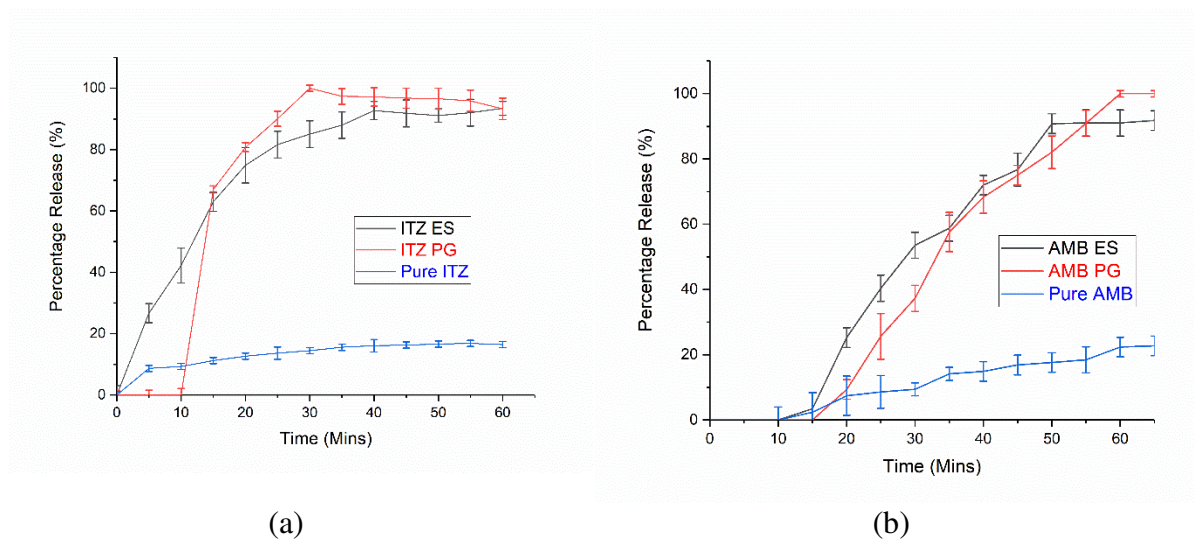


Figure 8. (Drug dissolution profiles (a) Itraconazole-loaded fibers (b) amphotericin B fibers.)

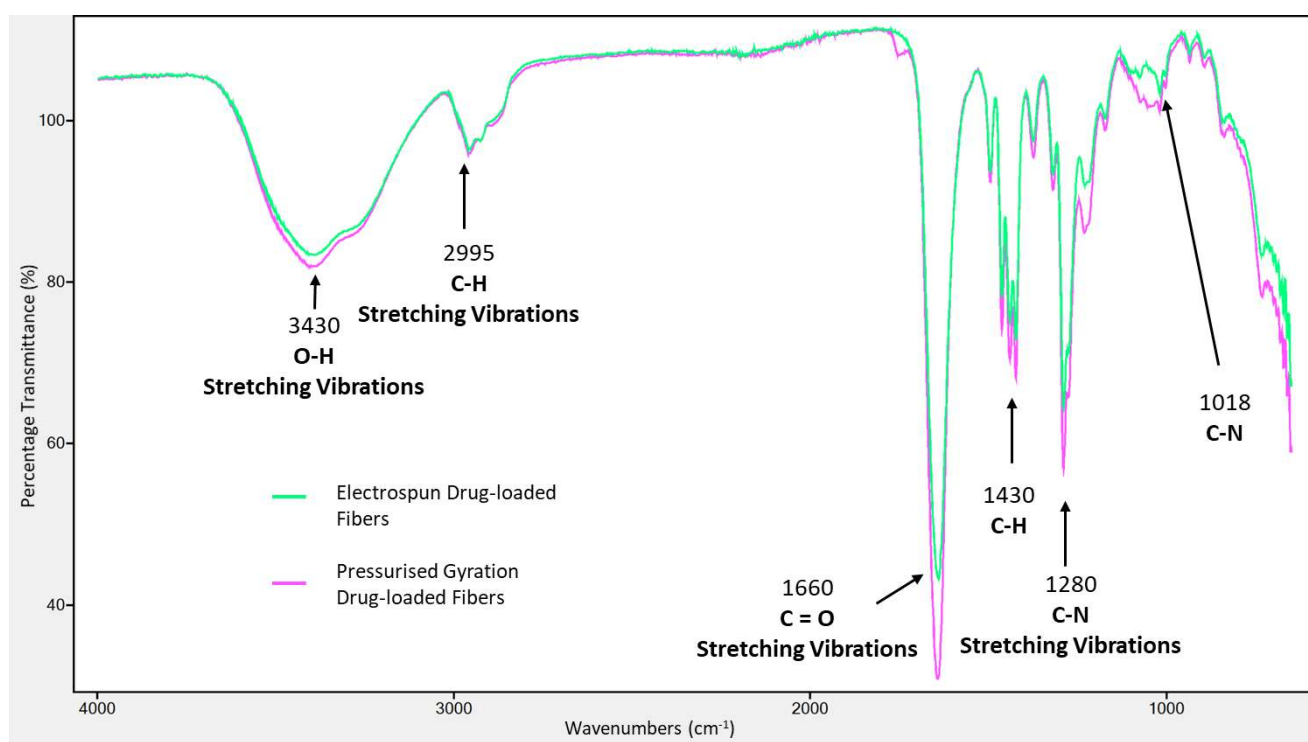


Figure 9. FTIR spectra for ES and PG itraconazole-loaded PVP fibres.

Table 1. Polymer solutions used in this work

Polymer	% (w/v)	Solvent system
PVP	10	Ethanol
PVDF	25	1:1 Dimethylformamide : Acetone
PMMA	20	Dichloromethane
PINIPAm	20	2:1 Chloroform : Ethanol

Table 2. Electrospinning and Gyration spinning conditions

Polymer	Electrospinning			Pressurised Gyration		
	kV	Flow rate ($\mu\text{l}/\text{min}$)	Collecting distance (mm)	Pressure (MPa)	Rotation speed (rpm)	Collecting distance (mm)
PVP	16.0	100	150	0.1	36000	120
PVDF	18.0	50	150	0.1	36000	120
PMMA	16.0	150	150	0.1	36000	120
PINIPAm	17.0	150	150	0.1	36000	120

Table 3: Average fibre diameters achieved

Polymer System	Average Fibre Diameter ($\pm \mu\text{m}$)	
	Electrospinning	Pressurised Gyration
PVP (Pure)	3.13 ± 1.34	3.53 ± 1.70
PVDF	4.63 ± 1.22	1.58 ± 0.76
PMMA	5.57 ± 2.11	1.97 ± 1.75
PNIPAm	3.00 ± 0.50	6.30 ± 3.60
PVP (Itraconazole)	0.94 ± 0.34	1.60 ± 0.87
PVP (AMP B)	0.88 ± 0.35	1.78 ± 0.81

Table 4: Polymer solutions used

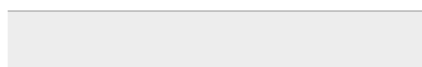
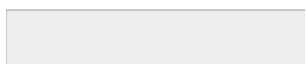
Polymer Solution	Surface Tension (mNm^{-1})	Viscosity ($\text{mPa} \cdot \text{s}$)
PVP (Ethanol)	21.6 ± 0.9	476.3
PVDF (1:1 Dimethylformamide : Acetone)	28.1 ± 0.5	475.4

PMMA (Dichloromethane)	26.8 ± 0.4	27.6
PINIPAm (2:1 Chloroform: Ethanol)	83.0 ± 1.5	654.1

1
2
3
4
5
6
7
8
9
10
11
12
13
14
15
16
17
18
19
20
21
22
23
24
25
26
27
28
29
30
31
32
33
34
35
36
37
38
39
40
41
42
43
44
45
46
47
48
49
50
51
52
53
54
55
56
57
58
59
60
61
62
63
64
65

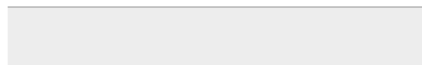
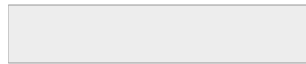


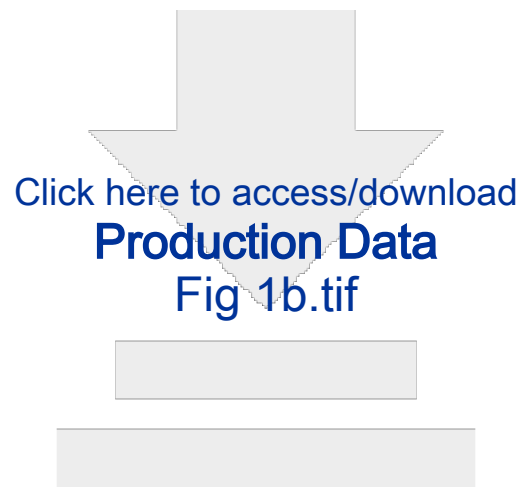
Click here to access/download
Production Data
Abstract.tif





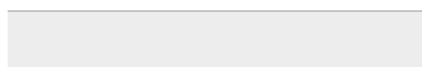
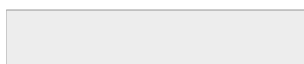
Click here to access/download
Production Data
Fig 1a.tif





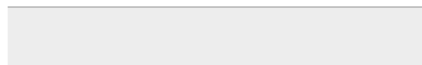
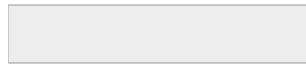


Click here to access/download
Production Data
Fig 2.tif



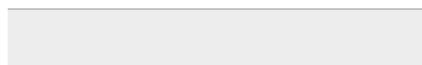
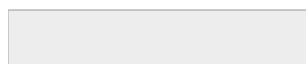


Click here to access/download
Production Data
Fig 3.tif



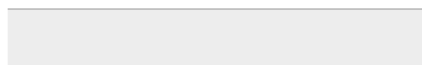
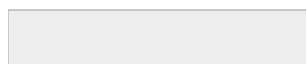


Click here to access/download
Production Data
Fig 4.tif



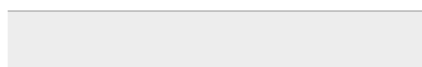
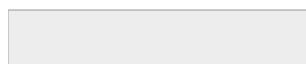


Click here to access/download
Production Data
Fig 5.tif



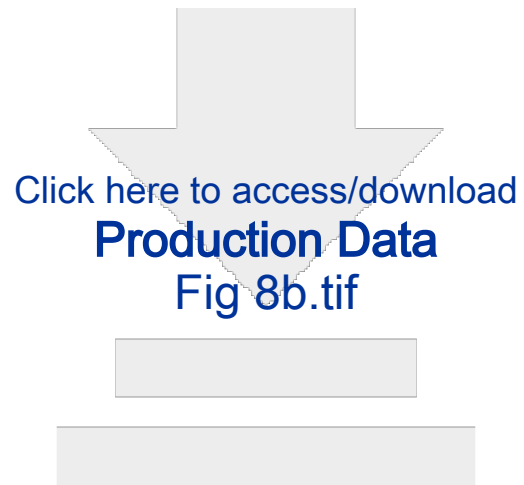


Click here to access/download
Production Data
Fig 6.tif











Click here to access/download
Production Data
Fig 9.tif

